Discrete analysis of Schwarz Waveform Relaxation for a simplified air-sea coupling problem with nonlinear transmission conditions

Simon Clement, Florian Lemarié, Eric Blayo

Discrete analysis of Schwarz Waveform Relaxation for a simplified air-sea coupling problem with nonlinear transmission conditions

S. Clement, F. Lemarié, and E. Blayo

1 Introduction

Schwarz-like domain decomposition methods are very popular in mathematics, computational sciences and engineering notably for the implementation of coupling strategies. Such an iterative method has been recently applied in a state-of-the-art Earth System Model (ESM) to evaluate the consequences of inaccuracies in the usual ad-hoc ocean-atmosphere coupling algorithms used in realistic models [2]. For such a complex application it is challenging to have an a priori knowledge of the convergence properties of the Schwarz method. Indeed coupled problems arising in ESMs often exhibit sharp turbulent boundary layers whose parameterizations lead to peculiar transmission conditions. The objective in this paper is to study a model problem representative of the coupling between the ocean and the atmosphere, including discretization and so-called bulk interface conditions which are analogous to a quadratic friction law. Such a model is introduced in Sec. 2 and its discretization, as done in state-of-the-art ESMs, is described in Sec. 3. In the semi-discrete case in space we conduct in Sec. 4 a convergence analysis of the model problem first with a linear friction and then with a quadratic friction linearized around equilibrium solutions. Finally, in Sec. 5, numerical experiments in the linear and nonlinear case are performed to illustrate the relevance of our analysis.

S. Clement
S. Clement, Univ Grenoble Alpes, CNRS, Inria, Grenoble INP, LJK, Grenoble, France, e-mail: simon.clement@grenoble-inp.org

F. Lemarié
F. Lemarié, Univ Grenoble Alpes, Inria, CNRS, Grenoble INP, LJK, Grenoble, France, e-mail: florian.lemarie@inria.fr

E. Blayo
E. Blayo, Univ Grenoble Alpes, CNRS, Inria, Grenoble INP, LJK, Grenoble, France, e-mail: eric.blayo@univ-grenoble-alpes.fr

2 Model problem for ocean-atmosphere coupling

We focus on the dynamical part of the oceanic and atmospheric primitive equations and neglect the horizontal variations of the velocity field, which leads to a model problem depending on the vertical direction only. This assumption, commonly made to study turbulent mixing in the boundary layers near the air-sea interface, is justified because of the large disparity between the vertical and the horizontal spatial scales in these layers. We consider the following diffusion problem accounting for Earth's rotation (f is the Coriolis frequency and $\mathbf{k}$ a vertical unit vector):

$$\begin{cases} \partial_t \mathbf{u} + f\mathbf{k}\times\mathbf{u} - \partial_z\left(\nu(z,t)\partial_z\mathbf{u}\right) = \mathbf{g}, & \text{in } \Omega\times(0,T), \\ \mathbf{u}(z,0) = \mathbf{u}_0(z), & \forall z \text{ in } \Omega, \\ \mathbf{u}(H_o,t) = \mathbf{u}_o^\infty(t),\ \mathbf{u}(H_a,t) = \mathbf{u}_a^\infty(t), & t\in(0,T), \end{cases}$$

with $\mathbf{u} = (u,v)$ the horizontal velocity vector, $\nu(z,t) > 0$ the turbulent viscosity and $\Omega = (H_o, H_a)$ a bounded open subset of $\mathbb{R}$ containing the air-sea interface $\Gamma = \{z = 0\}$. In the ocean and the atmosphere, which are turbulent fluids, the velocity field varies considerably in the few meters close to the interface (in a region called *surface layer*). The cost of an explicit representation of the surface layer in numerical simulations being unaffordable, this region is numerically accounted for using wall laws a.k.a. log laws (e.g. [4]). This approach, traditionally used to deal with solid walls, is also used in the ocean-atmosphere context, with additional complexity arising from the stratification effects [5]. In this context wall laws are referred to as *surface layer* parameterizations. The role of such parameterizations is to provide $\nu\partial_z\mathbf{u}$ on the upper and lower interfaces of the surface layer as a function of the difference of fluid velocities. Thus the coupling problem of interest should be understood as a domain decomposition with three non-overlapping subdomains. For the sake of convenience the velocity vector $\mathbf{u} = (u,v)$ is rewritten as a complex variable $U = u + iv$. Then the model problem reads

$$\begin{aligned} \partial_t U_j + ifU_j - \partial_z\left(\nu_j(z,t)\partial_z U_j\right) &= g_j, \qquad (j = o,a) && \text{in } \Omega_j\times(0,T) \\ U_j(H_j,t) &= U_j^\infty(t), && t\in(0,T), \\ U_j(z,0) &= U_0(z), && \forall z \text{ in } \Omega_j, \\ \rho_o\nu_o\partial_z U_o(\delta_o,t) = \rho_a\nu_a\partial_z U_a(\delta_a,t) &= \mathcal{F}_{\text{sl}}(U_a(\delta_a,t) - U_o(\delta_o,t)), && t\in(0,T) \end{aligned} \tag{1}$$

where $\Omega_o = (H_o,\delta_o)$, $\Omega_a = (\delta_a, H_a)$, and $\mathcal{F}_{\text{sl}}$ is a parameterization function for the surface layer extending over $\Omega_{\text{sl}} = (\delta_o,\delta_a)$. A typical formulation for $\mathcal{F}_{\text{sl}}$ is

$$\mathcal{F}_{\text{sl}}(U_a(\delta_a,t) - U_o(\delta_o,t)) = \rho_a C_D |U_a(\delta_a,t) - U_o(\delta_o,t)|(U_a(\delta_a,t) - U_o(\delta_o,t))$$

which corresponds to a quadratic friction law with C_D a drag coefficient (assumed constant in the present study). Geostrophic winds and currents are used in this study as source terms and boundary conditions. Geostrophic equilibrium is the stationary state for which the Coriolis force compensates for the effects of gravity. It corresponds to the large scale dynamics of ocean and atmosphere, and leads to reasonable values of the solution U.

The well-posedness of (1) has been studied in [6] where it is proved that its stationary version admits a unique solution for realistic values of the parameters. The study of the nonstationary case is much more challenging: numerical experiments tend to confirm this well-posedness, but with no theoretical proof.

3 Discretized coupled problem

3.1 Implementation of the surface layer

As described in Sec. 2, the full domain Ω is split into three parts: Ω_o in the ocean, Ω_a in the atmosphere and $\Omega_{\rm sl}$ a thin domain containing the interface (see Fig. 1). The role of $\Omega_{\rm sl}$ is to provide $\rho_j \nu_j \partial_z U_j$ at $z = \delta_j$ $(j = o, a)$ as a function of fluid velocities at the same locations. However, in state-of-the-art climate models, the discretization is based on an approximate form of the coupled problem (1). For practical reasons, the computational domains are $\widetilde{\Omega}_o = (H_o, 0) = \Omega_o \bigcup (\delta_o, 0)$ and $\widetilde{\Omega}_a = (0, H_a) = (0, \delta_a) \bigcup \Omega_a$, and the locations of the lower and upper boundaries of the surface layer ($z = \delta_j$) are assimilated to the centers of the first grid cells (i.e. $\delta_o = -h_{\rm o}/2$ and $\delta_a = h_{\rm a}/2$ with $h_{\rm o}$ and $h_{\rm a}$ the thicknesses of the first grid cell in each subdomain), where the values of the velocity closest to the interface are available. Typical resolutions in the models are $\delta_a = h_{\rm a}/2 = 10$ m and $\delta_o = -h_{\rm o}/2 = -1$ m. At a discrete level, the transmission condition in (1) is replaced by

$$\rho_{\rm o}\nu_{\rm o}\partial_z U_{\rm o}(0,t) = \rho_{\rm a}\nu_{\rm a}\partial_z U_{\rm a}(0,t) = \rho_{\rm a}\alpha\left(U_{\rm a}\left(\frac{h_{\rm a}}{2},t\right) - U_{\rm o}\left(-\frac{h_{\rm o}}{2},t\right)\right) \quad (2)$$

where $\alpha = C_D \left|U_{\rm a}\left(\frac{h_{\rm a}}{2},t\right) - U_{\rm o}\left(-\frac{h_{\rm o}}{2},t\right)\right|$ for the *nonlinear* case. In the following, for the analysis in Sec. 4, we consider a *linear* friction where α is assumed constant and a quadratic friction *linearized* around equilibrium solutions.

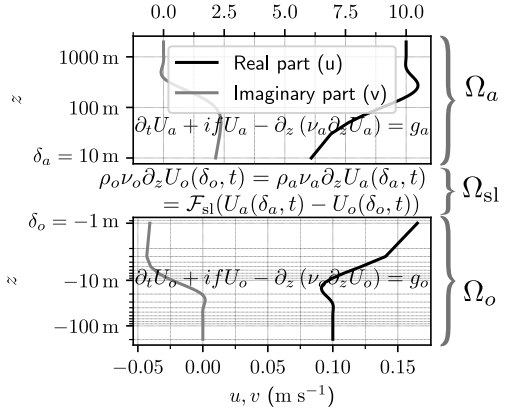

Fig. 1 Discrete representation of the three domains $\Omega_a, \Omega_{\rm sl}, \Omega_o$ together with a typical stationary state. Note the different scales for (u, v) in the ocean and in the atmosphere.

3.2 Schwarz Waveform Relaxation

As discussed for example in [2], current ocean-atmosphere coupling methods can actually be seen as a single iteration of a Schwarz Waveform Relaxation (SWR) algorithm. SWR applied to the coupling problem presented in Sec. 2 with the transmission conditions (2) and constant viscosity in each subdomain reads:

$$(\partial_t + if)U_j^k - \nu_j \partial_z \phi_j^k = g_j, \qquad \text{in } \widetilde{\Omega}_j \times (0,T) \tag{3a}$$

$$U_j^k(z,0) = U_0(z), \qquad \forall z \in \widetilde{\Omega}_j \tag{3b}$$

$$U_j^k(H_j,t) = U_j^\infty, \qquad t \in [0,T] \tag{3c}$$

$$\nu_{\mathrm{a}}\phi_{\mathrm{a}}^k(0,t) = \alpha^{k-1}\left(U_{\mathrm{a}}^{k-1+\theta}\left(\frac{h_{\mathrm{a}}}{2},t\right) - U_{\mathrm{o}}^{k-1}\left(-\frac{h_{\mathrm{o}}}{2},t\right)\right), \ t \in [0,T] \tag{3d}$$

$$\rho_{\mathrm{o}}\nu_{\mathrm{o}}\phi_{\mathrm{o}}^k(0,t) = \rho_{\mathrm{a}}\nu_{\mathrm{a}}\phi_{\mathrm{a}}^k(0,t), \qquad t \in [0,T] \tag{3e}$$

where $j = \mathrm{a}, \mathrm{o}$, $\phi_j = \partial_z U_j$, and $U_{\mathrm{a}}^{k-1+\theta} = \theta U_{\mathrm{a}}^k + (1-\theta)U_{\mathrm{a}}^{k-1}$ with θ a relaxation parameter (interpolation for $0 \leq \theta \leq 1$ or extrapolation for $\theta > 1$). At each iteration, (3e) ensures that the kinetic energy is conserved at the machine precision in the coupled system which is a major constraint for climate models. In (3d), the presence of the parameter θ makes it resemble to a Dirichlet-Neumann Waveform Relaxation algorithm. Indeed, if (3d) is replaced by $U_{\mathrm{a}}^k = \theta U_{\mathrm{o}}^{k-1} + (1-\theta)U_{\mathrm{a}}^{k-1}$ the DNWR algorithm is retrieved, as examined in the continuous case in [1] and in the discrete case in [3]. However (3d) involves both ϕ_{a}^k and $U_{\mathrm{a}}^{k-1+\theta}$: the θ parameter appears thus here within (close to Robin) condition ($\nu_{\mathrm{a}}\phi_{\mathrm{a}}(0) - \alpha\theta U_{\mathrm{a}}(h_{\mathrm{a}}/2) = \ldots$), i.e. the relaxation is not performed directly on the converging variable which leads to convergence properties different from the DNWR case, as shown in Sec. 4.

In the following, centered finite difference schemes in space are used with constant space steps h_j. Derivatives are $\phi_j(z,t) = \frac{U_j(z+h_j/2,t) - U_j(z-h_j/2,t)}{h_j}$ and the semi-discrete version of (3a) in the homogeneous case is

$$(\partial_t + if)U_j(z,t) = \nu_j \frac{\phi_j(z+h_j/2,t) - \phi_j(z-h_j/2,t)}{h_j} \tag{4}$$

4 Convergence analysis

In this section we conduct a convergence analysis of the SWR algorithm (3) first with α a constant and then in a more complicated case where the problem is linearized around its equilibrium solutions. In the following we systematically make the assumption that the space domain is of infinite size (i.e. $H_j \to \infty$) for the sake of simplicity.

Linear friction case ($\alpha = \mathrm{const}$) We assume in this paragraph that $\alpha = \alpha_c$ with

α_c a constant independent of U_j and we study the system satisfied by the errors (i.e. $g_j, U_0, U^\infty = 0$). The Fourier transform in time of the finite difference scheme (4) yields $\widehat{U}_{\rm a}(h_{\rm a}/2) = \nu_{\rm a}\frac{\widehat{\phi}_{\rm a}(h_{\rm a})-\widehat{\phi}_{\rm a}(0)}{i(\omega+f)h_{\rm a}}$ with $\omega \in \mathbb{R}$ the frequency variable. After simple algebra, the transmission condition (3d) in Fourier space expressed in terms of the $\widehat{\phi}_j$ is

$$\begin{aligned}\left(\frac{\chi_a\nu_a}{h_a} + \theta\alpha_c\right)\widehat{\phi}^k_{\rm a}(0) - \theta\alpha_c\widehat{\phi}^k_{\rm a}(h_a) =&(1-\theta)\alpha_c(\widehat{\phi}^{k-1}_{\rm a}(h_{\rm a}) - \widehat{\phi}^{k-1}_{\rm a}(0)) \\ &- \alpha_c\frac{h_a\nu_o}{h_o\nu_a}(\widehat{\phi}^{k-1}_{\rm o}(0) - \widehat{\phi}^{k-1}_{\rm o}(-h_{\rm o}))\end{aligned} \tag{5}$$

with $\chi_j = \frac{i(\omega+f)h_j^2}{\nu_j}$. A discrete analysis of the finite difference scheme (4) in the frequency domain (e.g. [7]) leads to $\widehat{\phi}^k_{\rm o}(-mh_{\rm o}) = A_k(\lambda_{\rm o}+1)^m$ and $\widehat{\phi}^k_{\rm a}(mh_{\rm a}) = B_k(\lambda_{\rm a}+1)^m$ with $\lambda_j = \frac{1}{2}\left(\chi_j - \sqrt{\chi_j}\sqrt{\chi_j+4}\right)$ and m the space index. The convergence factor of SWR is then the rate at which A_k or B_k tends to 0. Combining (5) with the Fourier transform in time of (3e), we get the evolution of B_k which eventually leads to the following convergence factor:

$$\xi = \left|\frac{B_k}{B_{k-1}}\right| = \left|\frac{(1-\theta)+\epsilon\frac{h_{\rm a}\lambda_{\rm o}}{h_{\rm o}\lambda_{\rm a}}}{\frac{\nu_{\rm a}\chi_{\rm a}}{\alpha_c h_{\rm a}\lambda_{\rm a}} - \theta}\right|, \tag{6}$$

where $\epsilon = \frac{\rho_{\rm a}}{\rho_{\rm o}} \approx 10^{-3}$ in the ocean-atmosphere context. Note that the convergence factor (6) differs significantly from the semi-discrete convergence factor $\xi_{\rm DNWR} = |1-\theta_{\rm DNWR}\,(1-\epsilon h_{\rm a}\lambda_{\rm o}/(\lambda_{\rm a}h_{\rm o}))|$ of the DNWR algorithm. Moreover, it can be found that

$$\lim_{(\omega+f)\to 0}\xi = \frac{1}{\theta}\left|1-\theta+\epsilon\sqrt{\frac{\nu_{\rm a}}{\nu_{\rm o}}}\right| = \xi_0, \qquad \lim_{(\omega+f)\to\infty}\xi = 0.$$

As $\omega + f \to 0$ the asymptotic value ξ_0 depends on θ: it is $+\infty$ for $\theta = 0$ (i.e. a fast divergence), and $\xi_0 = \epsilon\sqrt{\frac{\nu_{\rm a}}{\nu_{\rm o}}}$ for $\theta = 1$. When $\omega \to \infty$, the convergence factor tends to zero (i.e. the convergence is fast for high frequencies). Whatever ω, it can be shown that the value ξ_0 is an upper bound of the convergence factor when $\theta \le 1$ if $\sqrt{\frac{\nu_{\rm o}}{\nu_{\rm a}}} \le \frac{h_{\rm o}}{h_{\rm a}}$, the latter condition being easily satisfied. Since we have $\epsilon \approx 10^{-3}$, the convergence is fast for $\theta = 1$ whereas ϵ does not play any role for $\theta = 0$. The optimal parameter $\theta_{\rm opt}$ for low frequencies is $1 + \epsilon\sqrt{\frac{\nu_{\rm a}}{\nu_{\rm o}}}$ which is very close to 1.

Linearized quadratic friction case The analysis of the nonlinear quadratic friction case (i.e. with $\alpha = C_D \mid U_{\rm a}\,(h_{\rm a}/2,t) - U_{\rm o}\,(-h_{\rm o}/2,t)\mid$) cannot be pursued through a Fourier transform. We thus consider the linearization of the problem around a stationary state U^e_j, ϕ^e_j satisfying (1): assuming that $U^k_j(\pm h_j/2,t)$ is in a neighborhood of $U^e(\pm h_j/2)$, the modulus in α is non-zero and we can differentiate α. Differences with the stationary state are noted $\delta\phi^k_j = \phi^k_j(0,t) - \phi^e_j(0)$ and

$\delta U_j^k = U_j^k(\pm h_j/2, t) - U_j^e(\pm h_j/2)$. After some algebra, the linearized transmission operator reads

$$\begin{aligned}\nu_{\mathrm{a}}\delta\phi_{\mathrm{a}}^k = \alpha^e \Bigg(\left(\frac{3}{2} - \theta\right) \delta U_{\mathrm{a}}^{k-1} + \theta\, \delta U_{\mathrm{a}}^k - \frac{3}{2}\delta U_{\mathrm{o}}^{k-1} \\ + \frac{1}{2}\frac{U_{\mathrm{a}}^e - U_{\mathrm{o}}^e}{\overline{U_{\mathrm{a}}^e - U_{\mathrm{o}}^e}}\, \overline{\delta U_{\mathrm{a}}^{k-1} - \delta U_{\mathrm{o}}^{k-1}} \Bigg)\end{aligned} \tag{7}$$

with $\alpha^e = C_D\,|U_{\mathrm{a}}^e(h_{\mathrm{a}}/2) - U_{\mathrm{o}}^e(-h_{\mathrm{o}}/2)|$. Following the derivation in the previous paragraph, we find that the convergence factor ξ^q in the linearized quadratic friction case differs from one iteration to another (it is indeed a function of $\frac{\overline{B_{k-1}(-\omega)}}{B_{k-1}(\omega)}$). However, for $(\omega + f) \to 0$ the term $\frac{1}{2}\frac{U_{\mathrm{a}}^e - U_{\mathrm{o}}^e}{\overline{U_{\mathrm{a}}^e - U_{\mathrm{o}}^e}}\, \overline{\delta U_{\mathrm{a}}^{k-1} - \delta U_{\mathrm{o}}^{k-1}}$ vanishes, therefore the asymptotic convergence rate ξ_0^q is independent of the iterate:

$$\lim_{(\omega+f)\to 0} \xi^q = \frac{1}{\theta}\left|\frac{3}{2} - \theta + \frac{3}{2}\epsilon\sqrt{\frac{\nu_{\mathrm{a}}}{\nu_{\mathrm{o}}}}\right| = \xi_0^q, \qquad \lim_{(\omega+f)\to\infty} \xi^q = 0.$$

The convergence is fast for high frequencies, as in the linear friction case. However the optimal parameter for $(\omega + f) \to 0$ is here $\theta_{\mathrm{opt}}^q = \frac{3}{2} + \frac{3}{2}\epsilon\sqrt{\frac{\nu_{\mathrm{a}}}{\nu_{\mathrm{o}}}}$. It is different from the optimal parameter θ_{opt} obtained with linear friction: for typical values of the ocean-atmosphere coupling problem, θ_{opt}^q is close to $\frac{3}{2}$. The asymptotic value ξ_0^q is not an upper bound of the convergence factor but it is a good choice for θ_{opt}^q.

5 Numerical experiments

The aim of this section is to illustrate the influence of the parameter θ, in the linear and quadratic friction cases. The stationary state U_j^e is used to compute $\alpha_c = \alpha^e = C_D|U_{\mathrm{a}}^e(\frac{h_{\mathrm{a}}}{2}) - U_{\mathrm{o}}^e(\frac{h_{\mathrm{o}}}{2})|$ in the linear case. Parameters of the problem are taken as realistic: $C_D = 1.2 \times 10^{-3}$, the space steps are $\frac{h_{\mathrm{a}}}{2} = 10$ m, $\frac{h_{\mathrm{o}}}{2} = 1$ m, the time step is 60 s, the size of the time window T is 1 day ($1440\Delta t$) and the computational domains sizes are $H_o = H_a = 2000$ m (100 and 1000 nodes respectively in Ω_a and Ω_o). The Coriolis parameter is $f = 10^{-4}$ s^{-1} and the diffusivities are $\nu_{\mathrm{a}} = 1$ m^2 s^{-1}, $\nu_{\mathrm{o}} = 3 \times 10^{-3}$ m^2 s^{-1}. U_j^∞ are set to constant values of 10 m s^{-1} in the atmosphere and 0.1 m s^{-1} in the ocean, while the forcing terms $g_j = ifU_j^\infty$ and the initial condition $U_0(z) = U_j^e(z)$. SWR is initialized at the interface with a white noise around the interface value of the initial condition. Figure 2 shows the evolution of the error for two choices of θ. The theoretical convergence according to ξ_0 is also displayed: $\sup_\omega \xi$ is an upper bound of the L^2 convergence factor [6] and ξ_0 is an approximation of $\sup_\omega \xi$. Both ξ_0 and ξ_0^q are close to the convergence rate, with the exception of ξ_0^q that predicts much faster convergence than observed when $\theta = 1.5$. This shows that the maximum of the convergence factor is not reached when

$(\omega + f) \to 0$ in this case. Figure 2 confirms the results of Sec. 4: when considering $\alpha = \alpha_c$ constant, the fastest convergence is achieved when θ is close to 1, similarly to the DNWR algorithm. However this does not translate into the nonlinear case, which converges faster with $\theta = 1.5$. Figure 3 shows that the convergence behavior with the linearized transmission condition is similar to the nonlinear case. As expected the convergence is faster for $\theta = 1.5$ than for $\theta = 1$. We observed that those results are robust to changes in the values of the parameters in the range of interest. Linearized transmission conditions are hence relevant to study theoretically the convergence properties of our nonlinear problem.

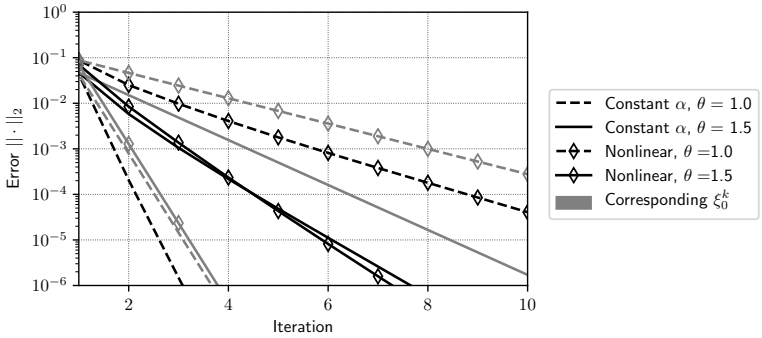

Fig. 2 Evolution of the L^2 norm of the errors. Black lines represent the observed convergence; grey lines are the estimated convergence with slopes ξ_0 for linear cases and ξ_0^q for quadratic cases.

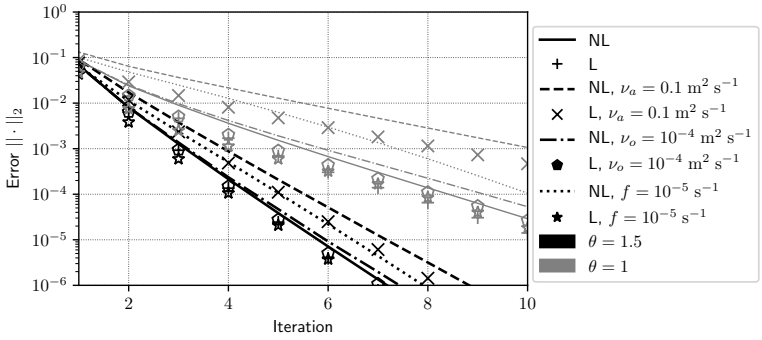

Fig. 3 Evolution of the L^2 norm of the errors with linearized (L) and nonlinear (NL) transmission conditions. The legend indicates the changes in the parameters for each case.

6 Conclusion

In this paper, we studied a SWR algorithm applied to a simplified ocean-atmosphere problem. This problem considers nonlinear transmission conditions arising from wall laws representative of the ones used in Earth-System Models and analogous to a quadratic friction law. We motivated the fact that the convergence analysis of such problems can only be done at a semi-discrete level in space due to the particular practical implementation of continuous interface conditions in actual climate models. Then we analytically studied the convergence properties in a case with linear friction and in a case with linearized quadratic friction. We formulated the problem with a relaxation parameter θ in the transmission conditions and systematically assessed its impact on the convergence speed. For the two cases of interest, the convergence factors are derived and the asymptotic limits for small values of the frequency $\omega + f$ are given. This asymptotic limit allowed us to choose appropriate values for the parameter θ to guarantee fast convergence of the algorithm. The behavior of the algorithm for linear friction and linearized quadratic friction turns out to be different which leads to different "optimal" values of θ. Numerical experiments in the nonlinear case showed that the observed convergence behaves as predicted by the linearized quadratic friction case whose thorough theoretical analysis is left for future work.

Acknowledgements This work was supported by the French national research agency through the ANR project COCOA (grant ANR-16-CE01-0007). Part of this study was carried out within the project PROTEVS under the auspices of French Ministry of Defense/DGA, and led by Shom.

References

1. Gander, M., Kwok, F., Mandal, B.: Dirichlet-Neumann and Neumann-Neumann waveform relaxation algorithms for parabolic problems. Electron. Trans. Numer. Anal. **45**, 424–456 (2016)
2. Marti, O., Nguyen, S., Braconnot, P., Valcke, S., Lemarié, F., Blayo, E.: A Schwarz iterative method to evaluate ocean–atmosphere coupling schemes: implementation and diagnostics in IPSL-CM6-SW-VLR. Geosci. Model Dev. **14**, 2959–2975 (2021)
3. Meisrimel, P., Monge, A., Birken, P.: A time adaptive multirate Dirichlet-Neumann waveform relaxation method for heterogeneous coupled heat equations. preprint arXiv:2007.00410 (2020)
4. Mohammadi, B., Pironneau, O., Valentin, F.: Rough boundaries and wall laws. Int. J. Numer. Methods Fluids **27**(1-4), 169–177 (1998)
5. Pelletier, C., Lemarié, F., Blayo, E., Bouin, M.N., Redelsperger, J.L.: Two-sided turbulent surface-layer parameterizations for computing air–sea fluxes. Quart. J. Roy. Meteorol. Soc. **47**(736), 1726–1751 (2021)
6. Thery, S.: Étude numérique des algorithmes de couplage océan-atmosphère avec prise en compte des paramétrisations physiques de couches limites. Phd thesis, Université Grenoble Alpes (2021). Https://tel.archives-ouvertes.fr/tel-03164786
7. Wu, S.L., Al-Khaleel, M.: Optimized waveform relaxation methods for RC circuits: Discrete case. Esaim Math. Model. Numer. Anal. **51**, 209–222 (2017)